Properties of TiN/CrN superlattice hard coatings deposited by reactive magnetron sputtering

IOP Conf. Series: Materials Science and Engineering **400** (2018) 032001 doi:10.1088/1757-899X/400/3/032001

Properties of TiN/CrN superlattice hard coatings deposited by reactive magnetron sputtering

M Angelov[1], T Cholakova[2], L Kolaklieva[3], R Kakanakov[4] and V Chitanov[5]
[1]Nanotech Group Ltd, 41, Nestor Abadzhiev Str., 4023, Plovdiv, Bulgaria
[2,3,4,5]Central Laboratory of Applied Physics, BAS, 61, St. Petersburg Blvd., Plovdiv, Bulgaria

E-mail: angelov@nanotech-group.com

Abstract. Nanostructured TiN/CrN superlattice hard coatings were deposited using a reactive closed field unbalanced magnetron sputtering in the presence of additional anode for higher plasma ionisation degree at temperatures lower than 240ºC. Coatings with three different bilayer periods (Λ) of 16 nm, 20 nm and 24 nm with applying a moderate substrate bias were obtained. The effect of bilayer period on the mechanical and tribological properties of the coatings was investigated by atomic force microscopy, nanoindentation, micro scratch and ball–on–disk wear tests. All the coatings possessed enhanced hardness, decreased coefficient of friction, improved adhesion and higher toughness in comparison with single-layer and gradient-composition hard coatings. The highest hardness value of about 30 GPa and elastic modulus of 360 GPa were measured for the coating with bilayer thickness of 24 nm. The friction coefficient against the diamond tip was within the range 0.2 for Λ=20 nm to 0,208 for Λ=16 nm. The calculated wear rates against 3/16 inch alumina ball were within the range from $1{,}045.10^{-6}$ $mm^3/N.m$ for Λ=24 nm to $1{,}955.10^{-6}$ $mm^3/N.m$ for Λ=16 nm. The static coefficient of friction μ_{SS} against polished SS plate was μ_{SS}=0,268 for Λ=24 nm, up to μ_{SS}=0,301 for Λ=16 nm, as the reference TiN layer possesses μ_{SS}=0,218. The wetting angle of the coatings against deionised water was between 91º for Λ=16 nm to 85º for Λ=24 nm.

1. Introduction

Superlattice coatings are multilayers, composed of alternating nanometer-thick layers of two different materials, as suggested by Koehler [1]. A variety of nanolayered multilayer coatings have been grown and studied [2-4] last three decades, because of their enhanced properties, such as high hardness [5], toughness and wear resistance [6], increased thermal stability [7], etc. Two main hardness enhancement mechanisms are suggested in the literature. The model of Chu and Barnett is based on hindering of the dislocation mobility within and between single layers with sharp interfaces and large enough difference in their shear moduli [8]. The model of Shinn and co-authors [9] explains the hardness enhancement with the difference in elastic modulus of the two layer materials and the coherency strain on the interfaces plays minor role. Recently the Chu and Barnett model is preferred because of better correlation with the experimental data.

TiN/CrN nanolayered multilayer coating is interesting because of its high hardness in the range of 32 - 38 GPa [7, 10, 11], preconditioned by the large difference in their shear moduli – 192 GPa for TiN and 125 GPa for CrN [10], toughness and wear resistance, high adhesion to the substrate, a low coefficient of friction and surface energy. As Barnett and Sproul suggested, the low lattice constant

mismatch (2,4%) between the cubic TiN and cubic CrN plays "epitaxial stabilization" role for the stoichiometric fcc CrN growth onto fcc TiN and suppresses Cr_2N formation [12]. Despite of it reactive sputter deposition of such a superlattice is a challenge because of the large difference in the heat of formation of CrN (29,8 kcal/mol) and TiN (80.8 kcal/mol) respectively [10,12]. Thus different nitrogen partial pressures during the CrN and TiN deposition are required. Although there are many studies of the mechanical and tribological properties of the superlattice coatings and TiN/CrN nanolayered multilayers in particular, a little is known for the wear and friction properties of these coatings. In this article are presented the results from investigation of the mechanical and tribological properties of TiN/CrN superlattice coatings as a function of the bilayer period, deposited by reactive Closed Field Unbalanced Magnetron sputtering, using an additional anode.

2. **Experimental**

Superlattice TiN/CrN coatings with different bilayer periods Λ were deposited by reactive Closed Field Unbalanced Magnetron pulsed DC sputtering and by use of additional anode for higher plasma volume and ionisation degree. Figure 1, shows the schematic diagram of the sputtering system. The working chamber is octagonal, 100 l by volume, 450 mm high. Turbomolecular pump based pumping unit provides base pressure of $2.0.10^{-4}$ Pa. Three unbalanced rectangular planar cathodes are mounted laterally through flanges on three of the chamber walls. Gas injection system with MKP digital mass-flow controllers is implemented in the cathodes, enabling feeding the Ar near to the targets and the reactive gases are directed to the substrates through the plasma volume. In our deposition system we used total pressure reactive gas control (the Ar flow and the total pressure of Ar + N_2 were kept constant during the deposition) and there is possible different nitrogen partial pressure to be set during the CrN and TiN single-layer deposition respectively. On both sides of the cathodes are mounted two additional water-cooled tubular anodes. On the chamber bottom is mounted a carousel with three-axial planetary mechanism. Rotation speed can be set within the range from 2 to 4.5 rpm, while the target to substrate distance is about 50 mm. All the power supplies are 2.0 kW MF pulsed DC, working on fixed 100 kHz and are remotely controlled. The magnetron power supplies work in power constant mode and provide the manufacturer's "new concept" [13] (see figure 2). On the door are mounted tubular heaters for substrates heating up to 400ºC during the deposition. The process is fully automated and provides options for creation, edition and saving of the technological recipes, based on Siemens series 1200 PLC and connected PC.

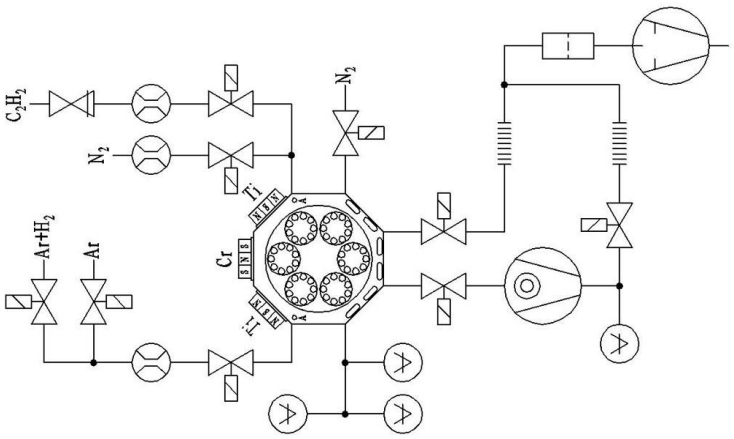

Figure 1. Schematic diagram of the sputtering HV system.

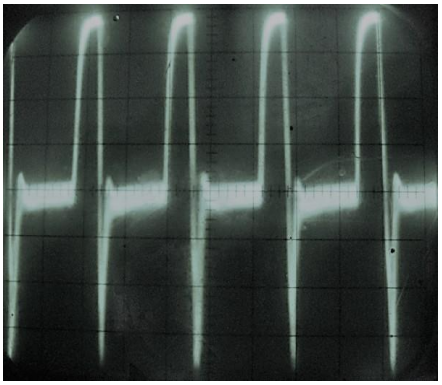

Figure 2. Pulse shape at real plasma load.

In our experiments two Ti targets were mounted on both lateral cathodes and one Cr target was mounted on the central ones. For all targets the material purity was 99.9% and the used gases purity was 99.996%. The samples were Φ20xD6 mm disks, made of hardened HSS, mirror polished and

cleaned by washing with alkali detergent, two-fold swill in ultrasonic baths in deionised water and vacuum dried at 210ºC. After loading and initial pumping up to 3.10^{-3} Pa, the samples were heated to 240ºC for 1 hour and after that cleaned in Ar glow discharge for 12 min. After glow discharge cleaning the working chamber was pumped to 1 – $1.5.10^{-3}$ Pa and samples were heated to 235ºC prior to ion etching in Ti^{+} ions for 10 min at Ar pressure $2,6.10^{-1}$ Pa, Ti cathodes power 1000 W and bias voltage –1000V. The additional anode voltage was +40V and was kept constant during the whole deposition process. After the ion etching the Ar gas pressure was set to $1.9.10^{-1}$ Pa, the bias voltage was decreased to -90V and kept constant during the rest of the process. The cathodes power was then increased to 1950W for 8 min for deposition of 200 nm Ti adhesion promoting sublayer, followed by 250 nm graded composition TiN_x + stoichiometric TiN layer at $2.1.10^{-1}$ Pa. It was followed by 450 nm graded composition $Ti_xCr_{1-x}N$ + $Ti_{0,48}Cr_{0,52}N$ layer by increasing the Cr target power to 1800 W, simultaneously with increasing the Nitrogen partial pressure to obtaining of $2.2.10^{-1}$ Pa total pressure before starting of multilayers deposition. This procedure was the same for all three processes.

The alternate TiN and CrN layers were deposited by fast switching “on” and “off” the Ti and Cr targets consecutively, with simultaneous change of the N_2 partial pressure for providing stoichiometric compound deposition, as in all coatings the last single layer was CrN. The achieved deposition rates were 12.48 nm/min for the CrN at $2.2.10^{-1}$ Pa total pressure and 11.52 nm/min for the TiN at $2.1.10^{-1}$ Pa total pressure onto three-fold rotating samples. These deposition rates were measured by deposition of single-layer TiN and CrN for 4 hours at the same process conditions and subsequent thickness measurement by a calotester. Different bilayer periods were obtained by changing the single layer deposition time, keeping constant target power and total working pressure. The coating with Λ=16 was deposited by 40 s long sequential runs of the related cathodes, while the 20 nm and 24 nm bilayers were deposited by 50 s and 60 s long target runs for 3 hours in all experiments.

The thickness measurements were made by manual calotester (Gencoa Ltd., Liverpool, UK) with 30 mm 100Cr6 ball and 100 nm diamond dispersion (Engis Ltd., UK), using optical microscope with 100x magnification and resolution of 0.01 mm. Surface morphology of the coating with Λ=20 nm bilayer period was studied by AFM, operated in non-contact mode. The mechanical properties of the deposited coatings were investigated using Compact Platform CPX (MHT/NHT) CSM Instruments equipment, Switzerland. The hardness measurements were performed by Nanoindentation module using a triangular pyramid Berkovich diamond indenter in the loading interval of 50 - 500 mN. The adhesion strength of the coatings to the substrate material and a friction coefficient were evaluated on the same equipment using Micro scratch module with a spherical Rockwell indenter with radius of 200 μm at progressively increasing load from 1 to 30 N. Wear tester for Ball-on-disk wear tests (Milko Angelov Consulting Co. Ltd.) was used for wear rate measurements against alumina ball. The wear track width was measured by optical microscope with 100x magnification and the wear volume was calculated, using geometric formulae. The static coefficient of friction against polished SS counterpart was measured by simple inclined plane with increased angle of inclination method. The wetting angle was measured by dripping of 25 μl deionised water onto the sample surface. High-resolution digital picture of it was taken and appropriate software to draw best-fit curve of the drop envelope and its tangent in the point of intersection with the sample surface was used. The angle between the tangent and the surface was then measured (see figure 3).

3. **Results and discussion**

3.1. Thickness measurements

Thickness measurement was essential in this study because of the chosen method for the multilayer coatings deposition and no other method for the bilayer period evaluation was used. By the manual calotester we made ball craters in the specimens and then measured their dimensions by optical microscope. Figure 4 shows the crater, made with Φ30 mm ball in the specimen surface. The layer thickness was calculated using the equation (1):

$$d = (R^2 - X^2)^{1/2} - (R^2 - Y^2)^{1/2} \quad (1)$$

where *R* is the ball radius, *X* is the inner circumference radius and *Y* is the outer circumference radius, *d* is the layer thickness, all values are in millimetres.

The control TiN single layer was 2.77 μm thick, while the control CrN single layer was 3.00 μm thick. All three multilayer coatings were 3.05 μm thick and for all measurements the resolution was 50 nm.

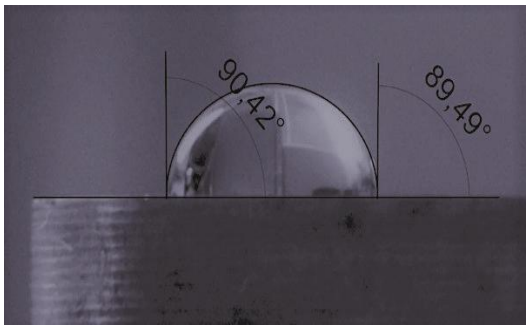

Figure 3. Wetting angle measurement illustration.

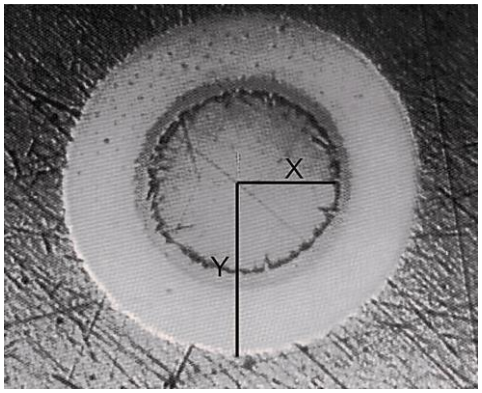

Figure 4. Ball crater for the full thickness measurement of the TiN/CrN-ml coatings.

3.2. Surface morphology

As it is well known [7, 12], the ion bombardment with moderate energy (70 – 90 eV) ions during the film growth suppresses the large grains formation and causes coating densification. Increasing the substrate bias voltage above –100 V increases the bombarded ion energy and re-sputtering occurs. This increases the defects formation, surface roughness and induced film stress. The 2D and 3D AFM images (figure 5a,b) of the coating with Λ=20 nm and thickness of 3,05 μm showed fine-grained structure and relevant smoothness, as no voids and cracks were evident. The measured values of the average roughness R_a=10,8 nm and root mean square roughness R_q=14,0 nm are close enough and show well packed surface with no defects. These roughness values are relatively higher in comparison with previously reported for a same coatings [10], but the coated specimens remain mirror smooth.

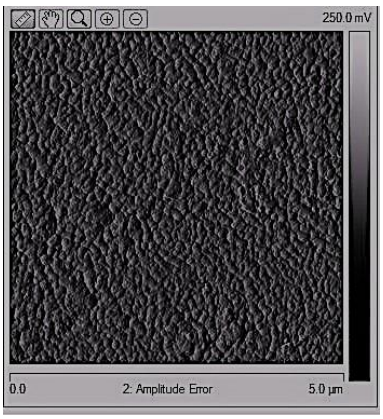

Figure 5a. 2D AFM image of the TiN/CrN-ml coating with Λ=20 nm.

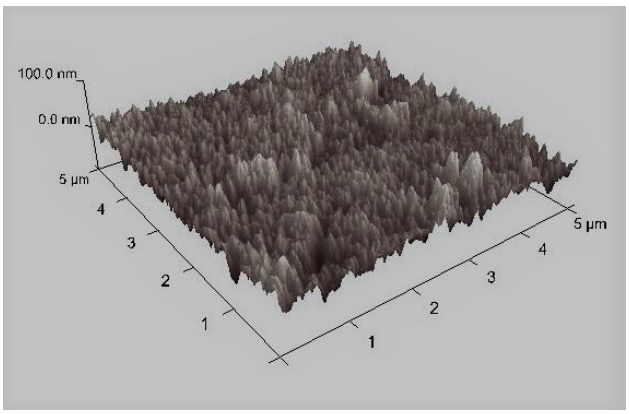

Figure 5b. 3D AFM image of the TiN/CrN-ml coating with Λ=20 nm.

3.3. Hardness measurements.

The nanohardness, indentation depth and elastic modulus values of the nanolayered multilayer coatings as a function of the applied load and the bilayer period Λ are shown in table 1. The properties of uncoated sample disk and TiN and CrN monolayer coatings obtained at 50 mN load are presented as references. The presented hardness and penetration depth values are average from ten indentations. Having in mind, that the penetration depths were about 12% of the coating thickness for 50 mN load, nanohardness values are affected by the substrate properties and thus slightly underestimated. Slight decrease in the measured hardness at 100 mN load, within 2 GPa was observed for all three coatings. At 200 mN load the hardness of the coatings remains 2.07 to 2.38 times higher in comparison with the not coated disk. Even at 500 mN load the hardness of the coating with Λ=24 nm is 1.82 times higher than that of not coated substrate, despite the penetration depth is 40% of the coating thickness. As it can be seen from the data, the coating with the highest bilayer period possesses the higher hardness for all loads, while the hardness of the coating with Λ=16 nm decreases stronger at higher loads.

Table 1: Hardness, Elastic modulus and indentation depth data as a function of the bilayer period.

Λ [nm]	$H_{0,05}$ [GPa]	$h_{0,05}$ [nm]	E [GPa]	$H_{0,1}$ [GPa]	$h_{0,1}$ [nm]	$H_{0,2}$ [GPa]	$h_{0,2}$ [nm]	$H_{0,5}$ [GPa]	$h_{0,5}$ [nm]
16	27.2	366	323	25.2	530	19.5	824	15.8	1395
20	27.9	360	332	26.0	527	21.0	790	16.9	1218
24	29.7	342	362	28.0	507	22.4	772	17.1	1210
TiN	23.0	397	306	-	-	-	-	-	-
CrN	16.4	453	289	-	-	-	-	-	-
UC disk	-	-	290	-	-	9.4	1065	-	-

In contrast with other superlattice studies, we measured highest hardness of about 30 GPa at bilayer period Λ=24 nm which is 2-6 times thicker, than the commonly reported [3-5, 7, 10, 12]. This result, together with the lower hardness value, can be explained with different hardening mechanism. We suppose, that the hardening is due to the crystallites size refinement to the hardest value for this bilayer period, as A.S. Argon [14] suggested, caused by the multilayer structure. Such behaviour can be explained with the not sharp enough interfaces between single TiN and CrN layers, caused by the simultaneous deposition of TiN and CrN during the switching on and off the cathodes for 4s and targets cross-contamination during the deposition. In our experiments about 5 s after switching on of the powered cathodes the process parameters showed the real change of the deposited material – this time is related to 12% of the single layer thickness for smallest bilayer period and 8% for the largest one. Another proof in this direction is the previously measured hardness of 27.4 GPa at 50 mN load for such a coating with bi-layer period Λ=30 nm, deposited onto the same substrate at the same conditions, measured in the same lab (not published). Despite of it, the rule-of-mixture value [7] for $Ti_{0,48}Cr_{0,52}N$ film would be about 19.6 GPa and the hardness enhancement for the hardest coating with Λ=24 nm is by factor of 1.52.

The analysis of the load – displacement curves at 50 mN load (figure 6) of the coatings shows that all three films have elastic recovery of about 50%. The last, together with the higher wear resistance, compared to single TiN layer, is important for forming applications, such as stamping and deep cold drawing.

3.4. Adhesion measurements

Scratch tests with R=0.2 mm hemispherical diamond tip under progressive load from 1 to 30 N were

performed for all three coatings to evaluate film adhesion. All three coatings showed excellent adhesion and similar results. Figure 7 shows a typical graphics of the scratch parameters for the coating with Λ=20 nm. While the friction force gradually increases with the applied normal load, the coefficient of friction curve remains flat and smooth, this means, that it is load independent. Figure 8a presents the scratch test patterns of the coating. The trace is smooth and no defects are evident up to about 24N, where very fine arc-shaped cracks appeared on the trace bottom (figure 8b), but up to 30 N delamination did not occurred, so L_{c2} was not reached. A possible reason for these values of L_{c1} is the compressive stress, affected by the intensive ion bombardment, together with the moderate substrates temperature during the deposition, but we did not studied stress values in this article.

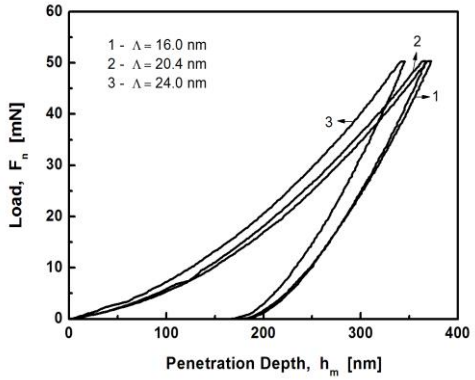

Figure 6. Load-displacement curves at 50 mN load.

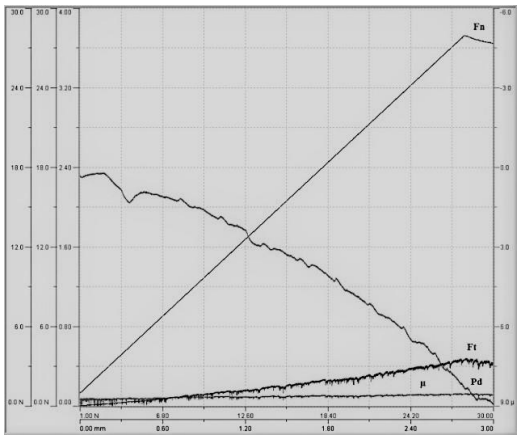

Figure 7. Friction force, coefficient of friction and penetration depth as a function of the normal load.

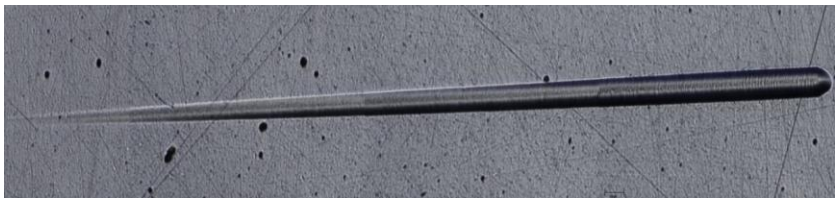

Figure 8a. Typical panoramic image of the scratch trace at the magnification x5.

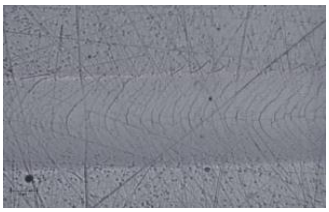

Figure 8b. Main part of scratch trace with critical load F_n=24N (L_{c1})

The measured values of the coefficient of friction against diamond tip are μ_D=0,2 for the film with Λ=20 nm, μ_D=0.208 for the coating with Λ=16 nm and μ_D=0.204 for the layer with Λ=24 nm. This behaviour cannot be explained based on this study and needs additional investigation.

We have studied the static coefficient of friction against polished SS counterpart as a function of the bilayer period Λ by inclined plate method, also. Ten measurements were made and average values were presented in table 2. These values are close to values, measured against the diamond tip. It is evident, that the friction decreases with increasing the bilayer period and the hardness of the coating. The static coefficient of friction of TiN against SS is presented as reference. We suppose that the lower coefficient of friction of TiN single layer is due to lower van der Waals forces in layer to SS plate interaction in comparison with the CrN last layer interaction with the same counterpart material. This can be explained with the 18% Cr content in the stainless steel 304L we used as a counterpart.

3.5. Wear rate measurements

Simple wear tester was used for these Ball-on-disk wear tests against 3/16 inch diameter alumina ball

at 5N constant load and 0,02 m/s sliding speed at 200 m sliding distance (5218 revolutions) for all measurements. The sliding speed was kept constant within ±0,5% of the adjusted value by feedback control, based on Siemens Simatic PLC and the sliding distance was reproducible within ±0,02% (one revolution). The friction force during the wear test was not measured. The wear track borderlines were smooth, no cracks, macroparticles or film delamination were observed. We measured the wear tracks width in eight points and average value was used in the calculations. No alumina ball wear was observed in all measurements. The wear track volume was calculated using the equation (2):

$$V = \pi D\{[2\pi R^2 \sin^{-1}(X/R)]/360 - X(R^2 - X^2)^{1/2}\} \quad (2)$$

where D=12.2 mm is the wear track average diameter, R=2.38 mm is the alumina ball radius and X is the wear track half-width in millimetres. The normalized wear rate is then calculated as, equation (3):

$$V_w = V/N.L \quad (3)$$

where V_w is the normalized wear rate in mm^3/Nm, V is the wear track volume in mm^3, N is applied normal load in Newtons and L is the sliding distance in meters. The measured values are shown in table 2. The wear rates of single-layered TiN and the uncoated disk were presented as references. The improvement in the wear rate in comparison with the reference TiN coating is by factor of 5,7 for the superlattice with Λ=24 nm, but even both softer multilayer coatings showed improved wear resistance. These values are in good correlation with the resistance to the plastic deformation (H^3/E^2) values and friction data for all coatings (see table 2).

Table 2. Wear rate, resistance to the plastic deformation, static coefficient of friction against SS counterpart and wetting angle data as a function of bilayer period.

Λ [nm]	V_w [mm^3/Nm]	H^3/E^2 [GPa]	μ_{SS}	Wetting angle [º]
16	$1.955.10^{-6}$	0.1929	0.301	90.4º
20	$1.342.10^{-6}$	0.1970	0.292	86.8º
24	$1.045.10^{-6}$	0.1999	0.268	85º
TiN	$5.963.10^{-6}$	0.130	0.218	58º
Uncoated disk	$5.958.10^{-5}$	0.0099	0.387	-

The measured wear rate values are in good agreement with those, reported by Rupetsov and co-authors in [15], where such nanostructured multilayer coating TiN/CrN – ml with bi-layer period Λ=30 nm, deposited in same HV system HVP100HRD onto hardened 1.2343 steel substrates, was studied by ball on plate method against 3 mm alumina bearings ball.

3.6. Wetting angle properties

The measured wetting angles of the multi-layered coatings (see table 2) are close, higher than that of TiN layer. It is evident, that the coating with lowest static coefficient of friction and the highest hardness possesses the lowest wetting angle and on the contrary - the film with smallest bilayer period and hardness showed highest wetting angle and slightly hydrophobic behaviour. It is important for applications, where the anti-sticking effect, together with enhanced wear resistance, is needed.

4. **Conclusions**

TiN/CrN nanolayered multilayer coatings with improved hardness, wear resistance and higher wetting angle in comparison with the reference TiN single layer were deposited by Closed Field Reactive Unbalanced Magnetron Sputtering at temperature of 235ºC. These coatings showed a maximum

hardness of 29.7 GPa, together with lower wear rate of $1{,}045.10^{-6}$ $mm^3/N.m$ at Λ=24 nm, while the coating with Λ=16 nm possesses slightly hydrophobic properties with 90.4º wetting angle. These coatings are appropriate for increasing the tool life of forming and stamping tools because of their lower friction, higher toughness and wear resistance. The coating with Λ=16 nm was used in plastics injection moulds as anti-sticking coating instead of TiN ones because of its hydrophobic behaviour, higher hardness and wear resistance and it resulted in longer periods before maintenance and longer tool life.

5. References

[1] Koehler J 1970 *Phys. Rev. B* **2** p 547
[2] Barnett S 1993 Deposition and properties of superlattice thin films. In: *Physics of thin films,* **17**, *Mechanic and dielectric properties*, eds. M. H. Francombe and J. S. Vossen, Academic Press Boston p 2
[3] Barnett S and Madan A 1998 *Phys. World* **11** p 45
[4] Munz W-D, Lewis D, Hovsepian P, Schonjahn C, Ehiasarian A and Smith I 2001 *Surf. Eng.* **17** p 15
[5] Shinn M, Hultman L and Barnett S 1992 *J. Mater. Res.* **7** p 901
[6] Ljungcrantz H, Engshtom E, Hultman L, Olsson M, Chu X, Wong M and Sproul W, 1998 *J. Vac. Sci. chnol. A* **16** p 3104
[7] Barshilia H, Jain A and Rajam K 2004 *Vacuum,* **72** p 241
[8] Chu X, Hultman L and Barnett S 1995 *J. Appl. Phys.* **77** p 4403
[9] Shinn M, Hultman L and Barnett S 1992 *J. Mater. Res.* **7** p 509
[10] Barshilia H and Rajam K 2003 *Bull. Mater. Sci.* **26**(2) p 233
[11] Yashar P, Barnett S, Rehner J and Sproul W 1998 *J. Vac. Sci. Technol. A* **16** p 2913
[12] Barnett S, Sproul W and Wong M 1996 *Deposition and properties of novel nitride superlattice coatings. Final report.* DOE/ERI 145434 – 5
[13] Angelov M 2007 *Proc. of International Conference NANOHARD 2007,* Velingrad, Bulgaria, May 13-16, p 101 ISBN 978-954-322-238-4
[14] Argon A 2008 *Strengthening mechanisms in Crystal Plasticity*, Oxford University, Oxford
[15] Rupetsov V, Kolaklieva L, Kopanov V, Chitanov V, Pashinski Ch and Dishliev S, 2015 *Journal of Food and Packaging Science, Technique and Technologies* **6** 91-95 ISSN 1314-7773